# Chapter 2

## Purification and characterization of mycolic acids and their methyl esters

### 2.1 Introduction

In order to investigate the properties and specific biological activities of the different subtypes of MAs in *M. tuberculosis*, they had to be separated. Different methods of separation have been described. Minnikin *et al.*, (48, 104) have used two-dimensional TLC to separate MAs into the different subclasses in order to determine specific patterns of MAs from different mycobacterial species for classification and identification.

Dubnau *et al.* (50) reported that the oxygenated MAs are necessary for virulence by infecting mice with a *M. tuberculosis* H37Rv strain and a mutant strain which is unable to synthesize oxygenated MAs. Yuan *et al.* (158) showed that not only the methoxy, but also the keto-function played an important role in cell wall function, as the *in vitro* growth of a *M. tuberculosis* strain lacking keto-mycolates was impaired at reduced temperatures and that glucose uptake was significantly reduced. The effect of INH did not change, but the sensitivity to ampicillin and rifampin increased. It could well be that each of the different subclasses of MA plays an important role in the sustenance and virulence of the organism.

### 2.2 Aim

It has been indicated that the immunological properties of the various subclasses of MA differ from one another (Chapter 1). In order to investigate this in more detail, pure fractions of each had to be prepared. This chapter describe the successful separation and then confirmation by structural analysis of the different subclasses of MAs harvested from *M. tuberculosis* H37Rv. The antigenicity of the different subtypes of natural MAs were then determined by using ELISA.

## 2.3 Esterification and separation of mycolic acids

### 2.3.1 Results and Discussion

#### *2.3.1.1 Preliminary experiments*

In order to exclude any factors that could influence the outcome of this experiment, the natural MAs that were isolated from *M. tuberculosis* H37Rv were analysed for purity. Analysis on HPLC gave a profile that corresponded with data reported in the literature. NMR spectra also corresponded with the data reported in literature, except that the sample contained some other minor components (150). To estimate the amount of these components in the natural MA sample, a small amount of the natural MA was loaded on a TLC plate which was developed, only once, using petroleum ether/ethyl acetate (4/1, v/v). The spots were visualized by dipping the plate into a molybdophosphoric acid (10%) solution in ethanol, followed by heating.

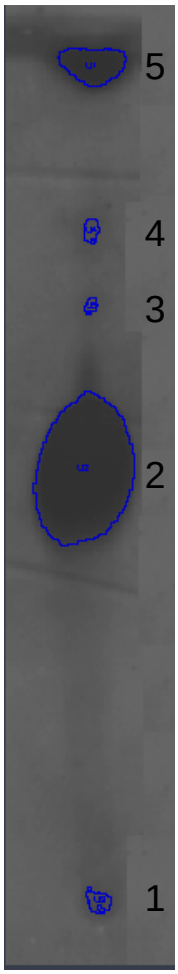


***Figure 2.1:*** *TLC of natural MAs and impurities from M. tuberculosis H37RV prepared in the laboratory.*

Then the dry TLC plate (Figure 2.1) was scanned and the results listed in Table 2.1. This confirmed that the sample contained less than 10% of other components.

***Table 2.1:*** *Analysis of the impurities in the sample of natural MAs from M. tuberculosis H37Rv prepared in the laboratory. Quantification of individual spots was carried out on a Versadoc (Model 3000) imaging system which measured the area and optical density of each spot. From this the density (optical density/area) and volume (Optical density*area) for each spot could be calculated. The values for the volume for each spot were given as % of the total.*

| Name | Area $mm^2$ | Density $ODu/mm^2$ | Volume $ODu*mm^2$ | % Vol. |
|---|---|---|---|---|
| 1 | 33.30 | 4.61 | 52.67 | 1.04 |
| 2 (Mycolic acids) | 976.76 | 5.28 | 1769.82 | 91.36 |
| 3 | 12.70 | 4.47 | 19.49 | 0.18 |
| 4 | 25.75 | 4.50 | 39.76 | 0.42 |
| 5 | 161.02 | 5.30 | 292.85 | 6.99 |

The $^{1}H$ NMR spectrum of the natural MAs showed a singlet at δ 3.34 for the methoxy-group (methoxy-MA), the proton next to the methoxy-group appeared as a multiplet at δ 2.96, the α-proton appeared as a double of triplets at δ 2.44 (*J* 5.4, 8.9 Hz). The *cis*-cyclopropane ring protons appeared as a multiplet at δ 0.65, a triplet of doublets at δ 0.57 (*J* 4.1, 8.2 Hz) and a broad double doublet at δ -0.33 (*J* 5.0, 8.9 Hz), the spectrum also showed two multiplets at δ 0.4 and δ 0.1 for the *trans*-cyclopropane ring protons. The $^{13}C$ NMR spectrum included a carbonyl signal at δ 176.21, a signal at δ 85.48 for the carbon next to the methoxy-group and at δ 57.72 for the carbon of the methoxy-group. The β-carbon appeared at δ 72.33, the α-carbon at δ 50.98 and the carbon next to the methyl group in the meromycolate chain appeared at δ 35.41. The spectrum showed signals for the carbons of the cyclopropane ring at δ 15.78 and δ 10.91.

Using a similar method to that described by Watanabe *et al.* (150, 151), it was possible to estimate the mycolate composition of the samples from NMR analyses (Table 2.2).

***Table 2.2:*** *Estimation of the ratios among the different subclasses from analyses of $^{1}H$ NMR spectrum of MAs.*

| **Signal** | | **Area** | **%** | **Ratios** |
|---|---|---|---|---|
| cyclopropane *cis* | | 1.36 | 93.04 | 1 |
| cyclopropane *trans* | | 0.10 | 6.51 | 0.08 |
| **3 different equations can be described:** | | | | |
| total cyclopropanes | = 2 (alpha) + 1 (methoxy) + 1 (keto) | 1.47 | | |
| H in β-position | = 1 (alpha) + 1 (methoxy) + 1 (keto) | 1 | | |
| H next to methoxy | = 1 (methoxy) | 0.51 | | |
| **From these 3 equations it was possible to estimate** | | | | |
| **Subclass** | | **Area** | **%** | **Ratios** |
| Alpha | | 0.465 | 46.54 | 1 |
| Methoxy | | 0.509 | 50.93 | 1.09 |
| Keto | | 0.025 | 2.53 | 0.05 |

*Explanation for the equations: Total cyclopropane = 2(alpha) + 1(methoxy) + 1 (keto): α-MA has 2 cyclopropanes, both cis, methoxy-MA and keto-MA have only 1 cyclopropane each, mostly cis, but trans as well. H in β position = 1(alpha) + 1(methoxy) + 1(keto): all 3 different subclasses have 1 proton on the β carbon. H next to methoxy = 1(methoxy): only methoxy-MA has a methoxy group in the meromycolate chain.*

The sample contained a negligible amount of double bond MAs, while *cis*- and *trans*-cyclopropanes were in a ratio equal to 1:0.08, and the ratios among α, methoxy and keto were equal to 1:1.09:0.05.

### *2.3.1.2 Esterification of natural mycolic acids*

According to Laval *et al.* (48, 93, 100, 101), MA may be separated into its different subgroups with TLC after it has been esterified with trimethylsilyl diazomethane (TMDM). The unmethylated MAs have a polar carboxylic acid group which strongly associates with the silica on the TLC plate causing the sample to smear, thus making separation incomplete. By methyl-esterification of the carboxylic acid, the MA subclasses separate simply due to the differences in functional groups in the meromycolate chain. The different subclasses were separated using a mobile phase containing 9:1 (v/v) petroleum ether:diethyl ether (147).

Twenty microlitres of the MA samples (10 mg/ml chloroform, *M. tuberculosis* MA batch A0698, MB - synthetic α-MA, kindly provided by Prof M.S. Baird (University of Wales, Bangor, UK); MA from Sigma; *M. tuberculosis* MA batch A1198) were incubated with 5µl of *n*-hexane-dissolved TMDM (2 M) at room temperature for one hour. The total volume of the TMDM incubated samples was loaded onto a silica plate that had been dried for two hours at

110 °C. After loading, the plate was dried briefly at 80 °C and then developed five times consecutively in a mobile phase containing 9:1 (v/v) petroleum ether:diethyl ether. Between developments, the plate was dried at 80 °C for ten minutes. Visualisation was done by sulfuric acid charring. Results are shown in Figure 2.2.

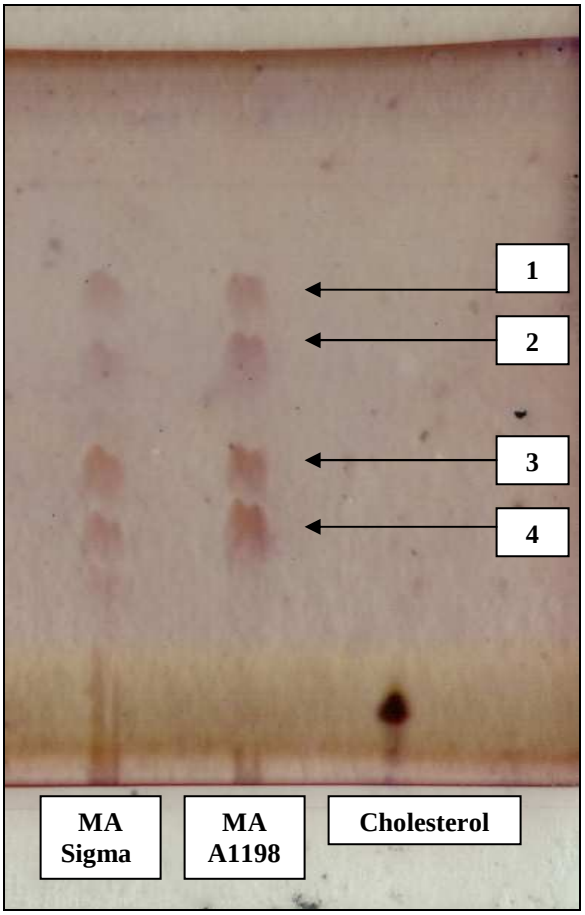


***Figure 2.2:*** *TLC of esterified MA from various sources (see text), compared to cholesterol. The four distinct spots in the MA lanes might be: 1 α-MA, 2 methoxy-MA, 3 keto-MA and 4 unesterified MA. (MA A1198 refers to a batch purified from M. tuberculosis by Sandra van Wyngaardt).*

Four distinct spots were observed after development with mobile phase. The $R_f$ values of the spots were (from bottom to top) 0.37, 0.48, 0.62 and 0.73. Three of these spots were expected to be the subclasses α-, keto- and methoxy-MA. The first spot was thought to be alpha-MA, as it is less polar than the oxygenated MAs, the second spot should then be methoxy and the third the keto-MA. Although the identity of the fourth (lowest) spot was unclear, it was thought to represent unesterified MA (Figure 2.2).

For the preparative TLC of the esterified MA, a total of 10 mg (ten times 10 µl of a 100 mg/ml chloroform solution) *M. tuberculosis* MA that had been esterified, was striped on a preparative TLC plate. The plate was developed as described, the sides removed and visualised by sulfuric acid charring before being compared with the remainder of the plate to identify the spots to be eluted (139, 150, 151). The different spots/fractions were eluted from the silica gel with chloroform, dried under nitrogen and submitted for NMR analysis. NMR analysis showed totally different results from what was expected.

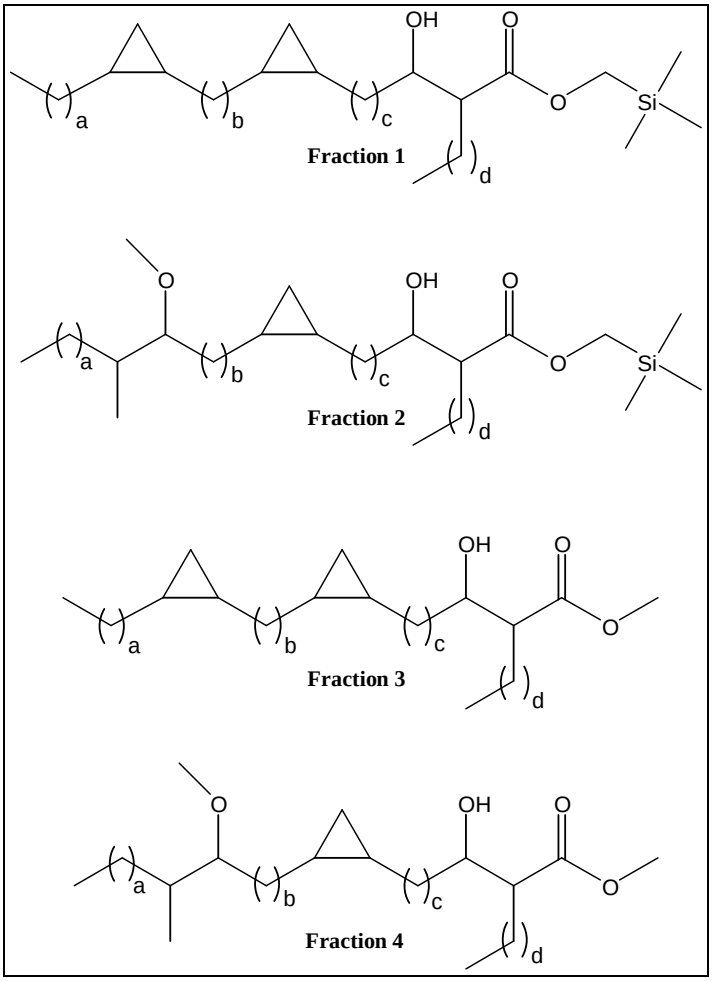


***Figure 2.3:*** *Structures of the different fractions of TLC separated natural MA determined by NMR analysis.*

Fraction 1 was indeed alpha-MA, but with a silyl group attached to the acid instead of a methyl, fraction 2 was methoxy-MA, also with a silyl group. Surprisingly, the third and fourth fractions were not keto- and unesterified MA, NMR showed it to be esterified α- and esterified methoxy MA. There was no detectable keto-MA present in any of the fractions (Figure 2.3).

Next, the esterification method of the MAs was reviewed. Trimethylsilyl diazomethane (TMDM) is a convenient methylating agent since it can be purchased commercially and is much safer to use than diazomethane. It is, however, important to include methanol in the solvent. Without methanol in the reaction, two products form, i.e. the methyl ester and trimethylsilyl methyl ester, which explains the products obtained previously (Figure 2.2). The methanol suppresses the following mechanism (Figure 2.4).

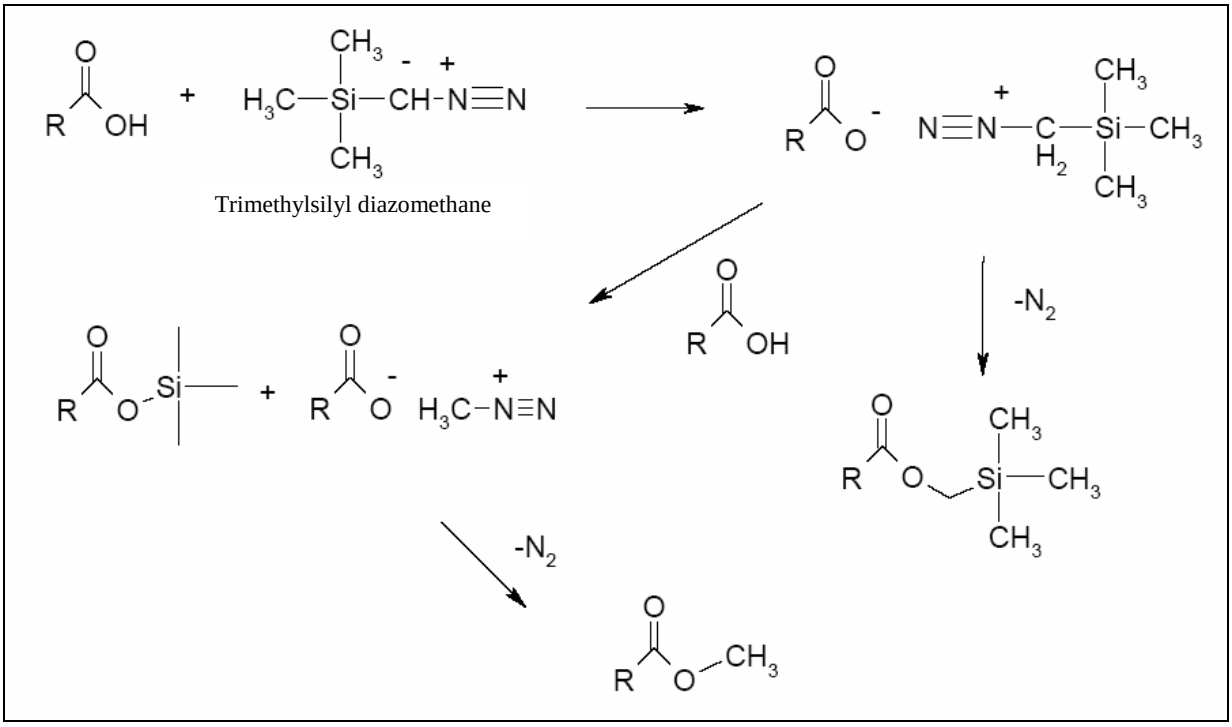


***Figure 2.4:*** *Reaction mechanism of trimethylsilyl diazomethane without methanol (132).*

The reaction of TMDM with carboxylic acids including methanol makes the reaction proceed according to the mechanism shown in Figure 2.5.

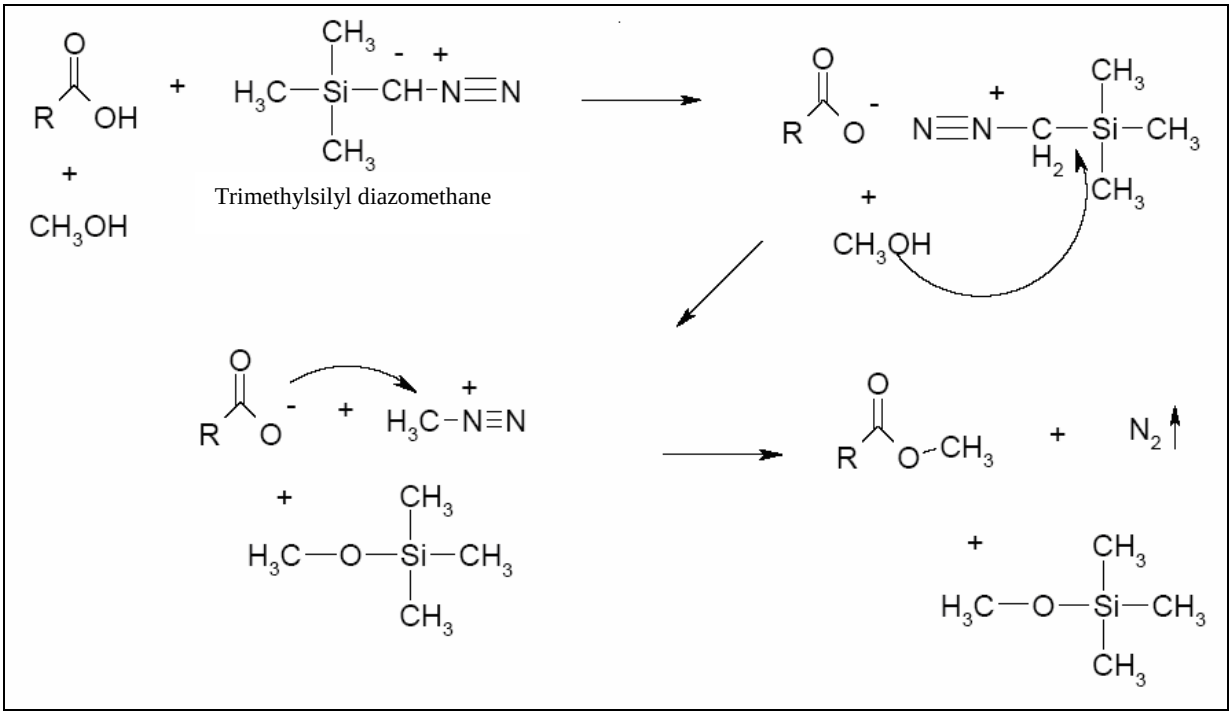


***Figure 2.5:*** *Reaction mechanism of trimethylsilyl diazomethane mediated methylesterification of carboxylic acids (132).*

In order to form the methyl esters, MAs were dissolved in a mixture of toluene and methanol (5:1) whereafter TMDM was added in a few small portions. After 72 hours of stirring, the reaction mixture was quenched and extracted with dichloromethane to give a high yield of 97% of mycolic acids methyl esters.

The $^{1}$H NMR spectrum of the esterified, unseparated natural MA corresponded to that reported in the literature for mycolic acid methyl esters (77, 132). It showed the same peaks present in the natural MAs before methylation and an additional singlet at δ 3.72 for the methyl group in the MA motif (Figure 2.6).

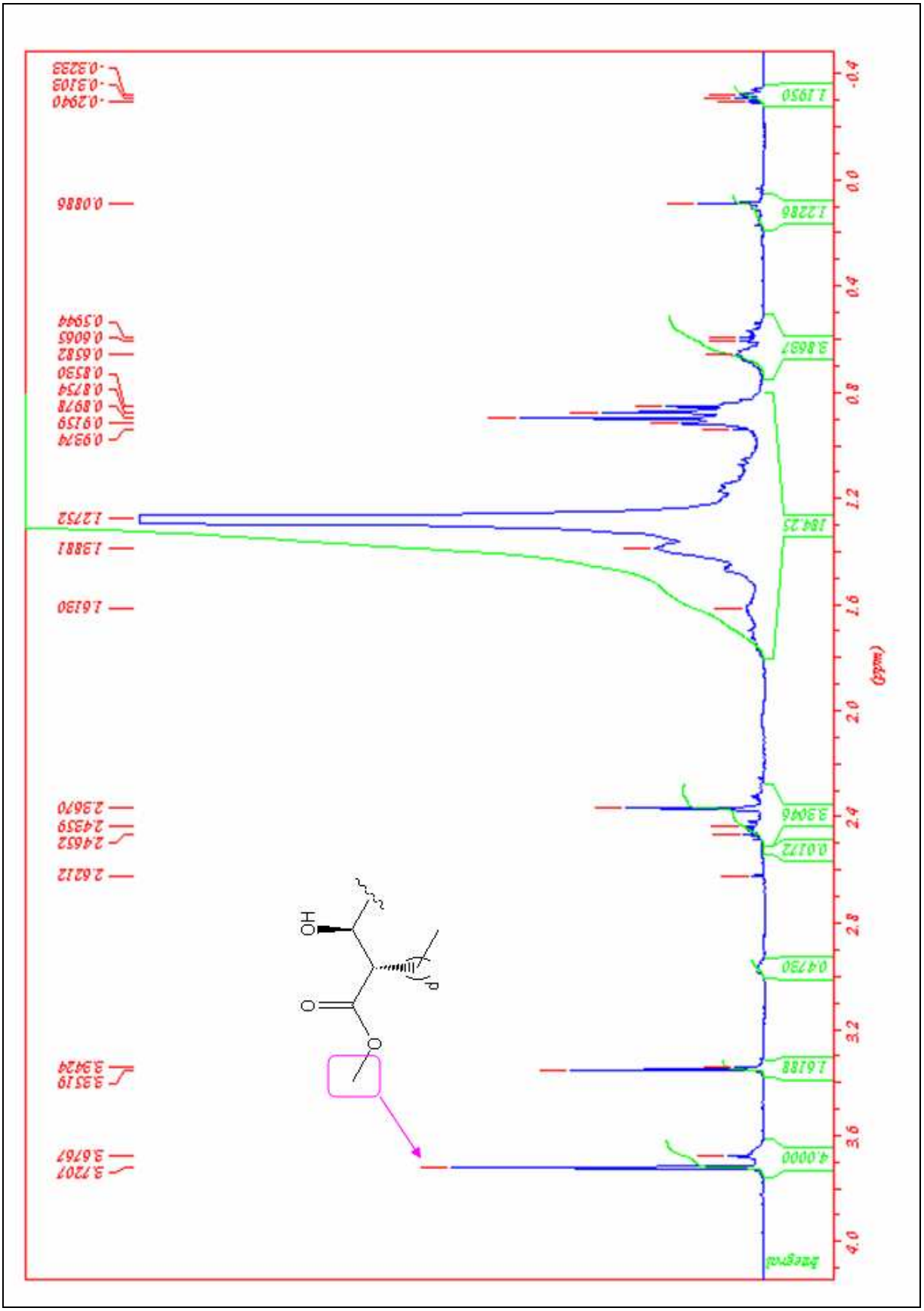


***Figure 2.6:*** *$^{1}$H NMR spectrum of natural mycolic acid methyl esters.*

TLC analysis of the product showed the presence of three spots. The spots were thought to be the three mycolic acid methyl ester subclasses (Figure 2.7).

After optimization, we were finally able to successfully separate the MAs into the three different subclasses after methylation of the natural MA. Separation of the different fractions of MAs was done by preparative TLC. Each fraction was purified by column chromatography, which eliminated all the impurities, except for the methyl keto-MA fraction which needed to be harvested and combined from more preparative TLC plates in order to come to a realistic yield for further work.

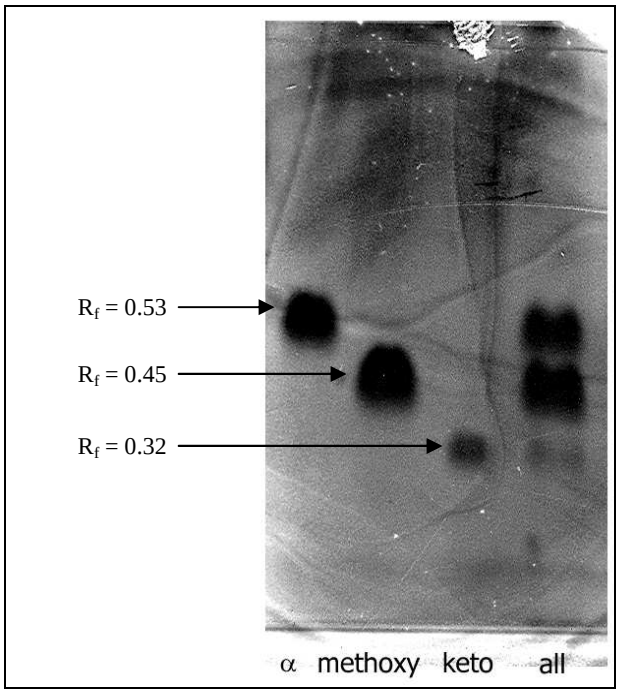


***Figure 2.7:*** *TLC of the different subclasses of mycolic acid methyl esters obtained after separation of the natural MA into the subclasses and extracted from preparative TLC plates. Lane 1 α-MA, lane 2 methoxy-MA, lane 3 keto-MA and lane 4 natural MA before separation.*

TLC confirmed the presence of alpha mycolic methyl ester ($R_f$ = 0.53), methoxy mycolic acid methyl ester ($R_f$ = 0.45) and keto mycolic acid methyl ester ($R_f$ = 0.32) as shown in Figure 2.7 [lit. respectively $R_f$ = 0.50, 0.46 and 0.36 (93)]. The quantification of individual spots showed that alpha:methoxy:keto mycolic acid methyl esters were in ratios of 1:1.29:0.06 (Table 2.3), which was in agreement with the results previously found by NMR analysis (Table 2.2).

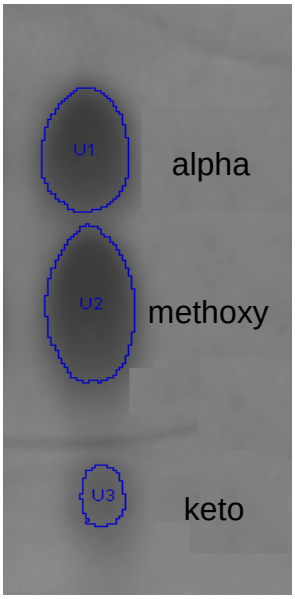


***Figure 2.8:*** *TLC, showing the different subclasses, used to determine the ratios of the different subclasses by spot quantification. TLC was performed on Silica Gel 60 using petroleum ether/ethyl acetate (4/1, v/v); lipid spots were revealed by dipping the plates into a molybdophosphoric acid (10%) solution in ethanol, followed by heating.*

***Table 2.3:*** *Estimation of the ratios amongst the different subclasses. Quantification of individual spots was done on a Versadoc (Model 3000) imaging system which measured the area and optical density of each spot. From this the density (optical density/area) and volume (optical density*area) for each spot could be calculated. The values for the volume for each spot were given as % of the total. From this the ratios were calculated.*

| Name | Area mm2 | Density ODu/mm2 | Volume ODu*mm2 | % Adj. Vol. | Ratios |
|---|---|---|---|---|---|
| alpha | 357.74 | 4.67 | 573.34 | 42.26 | 1 |
| methoxy | 448.38 | 4.69 | 721.33 | 54.32 | 1.29 |
| keto | 90.98 | 3.91 | 121.98 | 3.42 | 0.06 |

After purification the amounts of the different fractions recovered (Table 2.4) were comparable to the results calculated from the NMR spectrum (Table 2.2) and to the results of the spot quantification (Table 2.3 and Figure 2.8)

***Table 2.4:*** *The quantities of different fractions recovered.*

| Type of MA | mg extracted | Ratio among different fractions after extraction |
|---|---|---|
| α | 44.4 | 1 |
| Methoxy | 49.5 | 1.1 |
| Keto | 1.8 | 0.04 |

It is clear from the NMR and TLC analysis that the MAs isolated from *M. tuberculosis* H37Rv gave a higher percentage of methoxy-MA and a much lower percentage of keto-MA than reported in literature (93, 149, 150), where all three subclasses were found in approximately equal amounts.

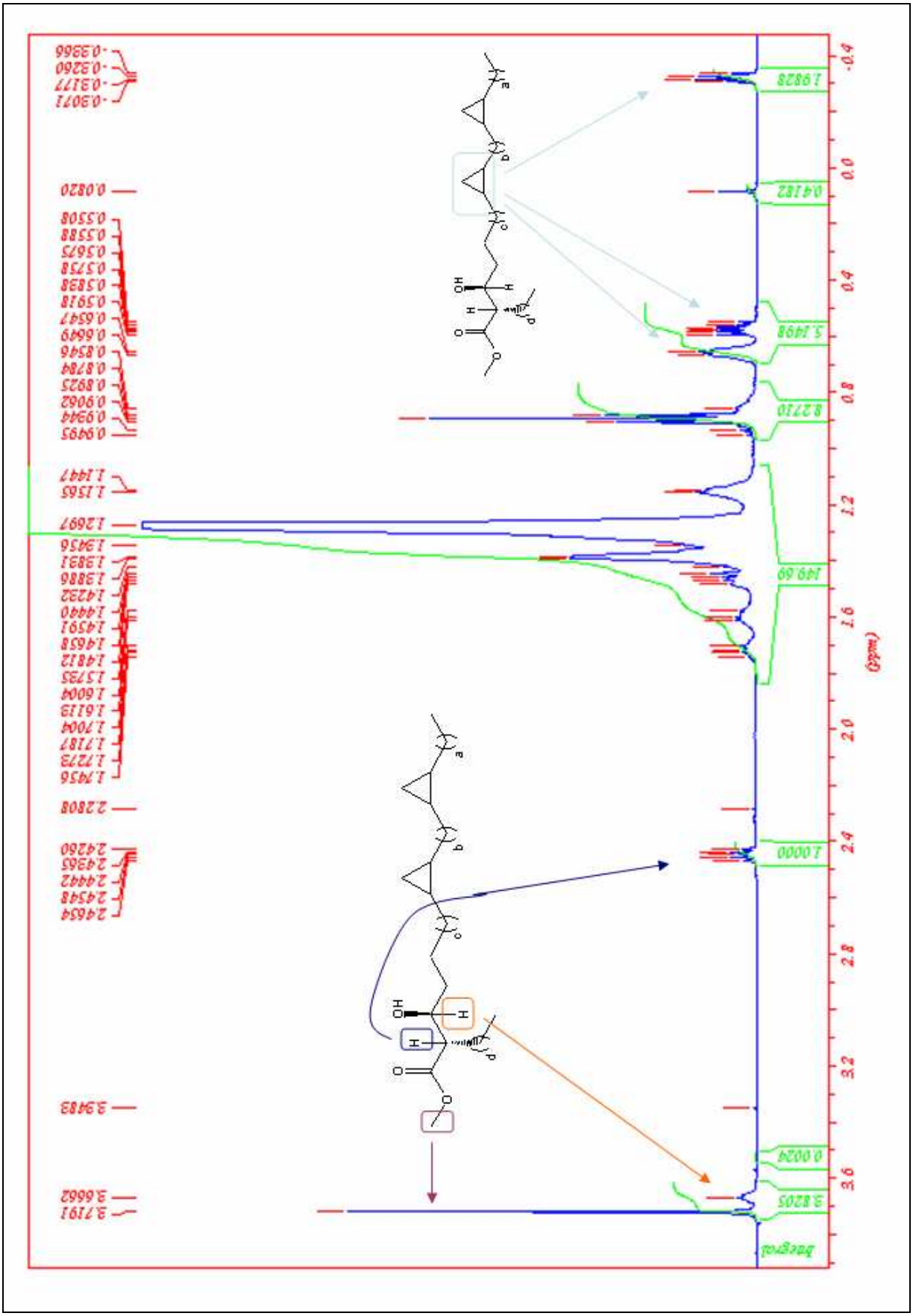

***Figure 2.9:*** *$^{1}$H NMR spectrum of α mycolic acid methyl ester.*

The $^{1}$H NMR spectrum of the α mycolic acid methyl ester showed a singlet at δ 3.72 for the methyl group in the mycolic acid motif. The β-proton appeared as a multiplet at δ 3.66 and the α-proton as a double of triplets at δ 2.44. The *cis*-cyclopropane ring protons appeared as a multiplet at δ 0.65, a triplet of doublets at δ 0.57 (*J* 4.1, 8.2 Hz) and another multiplet at δ -0.33 (Figure 2.9). The $^{13}$C NMR spectrum included a carbonyl signal at δ 176.20 and a signal at δ 51.47 for the carbon of the methyl group in the mycolic acid motif. The β-carbon appeared at δ 72.32 and the α-carbon at δ 51.00. The spectrum showed signals for the carbons of the cyclopropane ring at δ 15.80 and 10.94 (Figure 2.10).

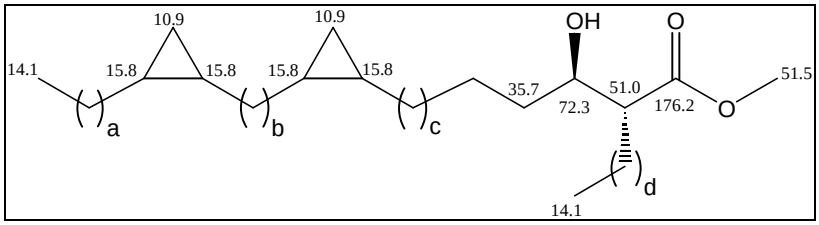


***Figure 2.10:*** *α mycolic acid methyl ester with $^{13}$C signals. Chemical shifts are quoted in δ relative to the trace resonance of $CDCl_3$ (δ 77.0 ppm).*

The NMR spectrum also showed minute amounts of impurities (1:191), as shown in Figure 2.11, which showed a peak at δ 3.35. These belong to methoxy-MA.

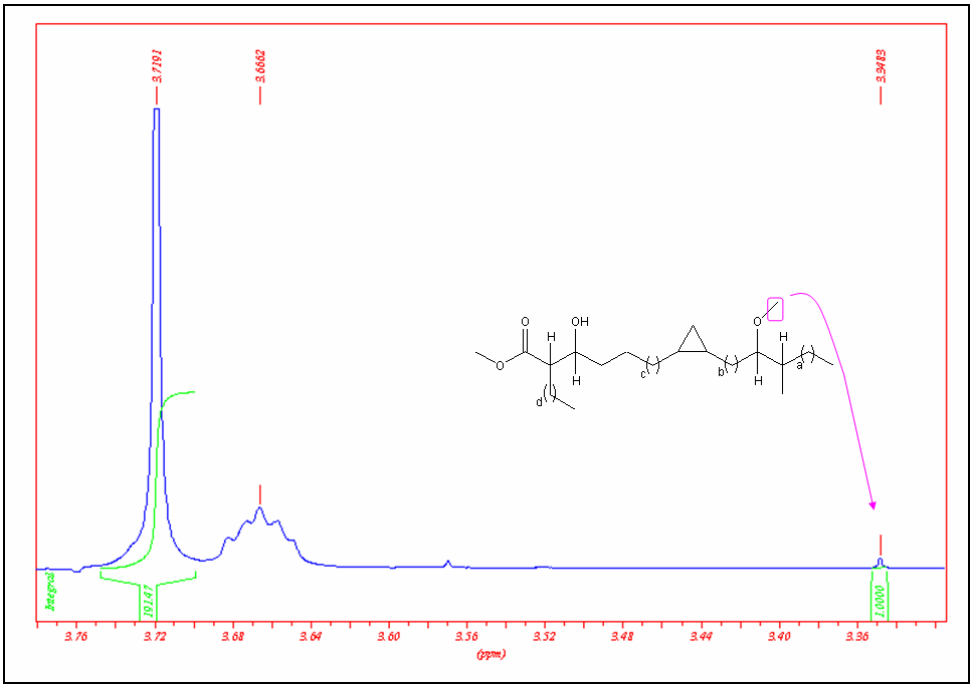


***Figure 2.11:*** *$^{1}$H NMR of alpha mycolic acid methyl ester showing impurities from methoxy mycolic acid methyl ester.*

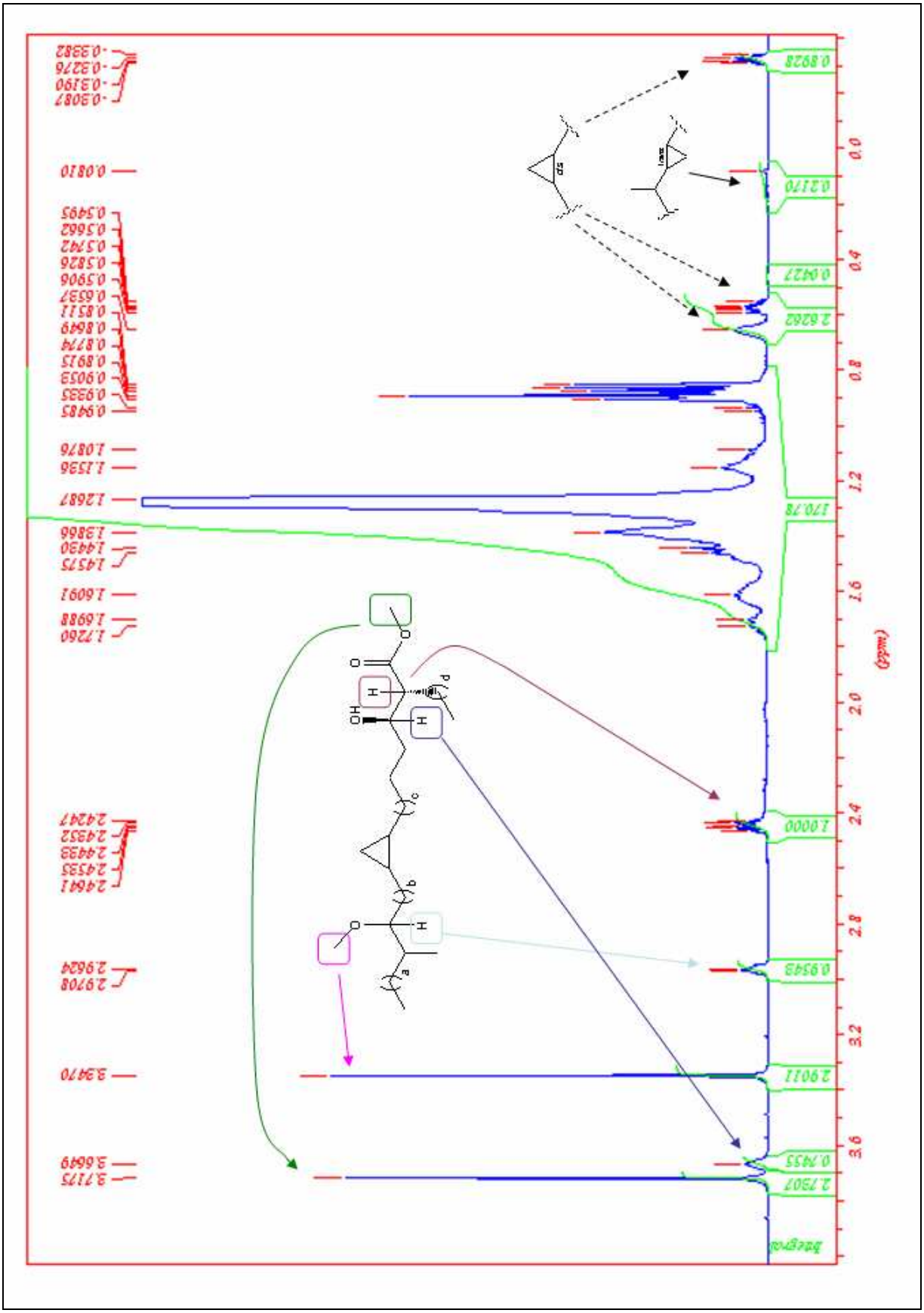

***Figure 2.12:*** *$^{1}$H NMR spectrum of methoxy mycolic acid methyl ester.*

The $^{1}$H NMR spectrum of the methoxy mycolic acid methyl ester showed a singlet at δ 3.72 for the methyl group in the mycolic acid motif, a multiplet at δ 3.66 for the proton on the β-carbon and a double of triplets at δ 2.44 (*J* 5.3, 9.2 Hz) for the proton of the α-carbon. The protons of the methoxy-group in the meromycolate chain appeared as a singlet at δ 3.32 and the proton next to the methoxy-group as a multiplet at δ 2.96. The spectrum showed a multiplet at δ 0.65, a triplet of doublets at δ 0.57 (*J* 4, 8.2 Hz) and a multiplet at δ -0.33 for the *cis*-cyclopropane ring protons. The *trans*-cyclopropane ring protons appeared as multiplets at δ 0.45 and 0.02-0.0. The *trans*-cyclopropane was less than 6% (Figure 2.12). The $^{13}$C NMR spectrum included a carbonyl signal at δ 176.20, a signal at δ 85.47 for the carbon next to the methoxy-group and at δ 57.71 for the carbon of the methoxy-group. The β-carbon appeared at δ 72.32 and the α-carbon at δ 51.00. The carbons of the *cis*-cyclopropane ring appeared at δ 15.80 and 10.94, and the carbons of the *trans*-cyclopropane ring at δ 26.16, δ 18.62, δ 14.88 and δ 10.54 (Figure 2.13).

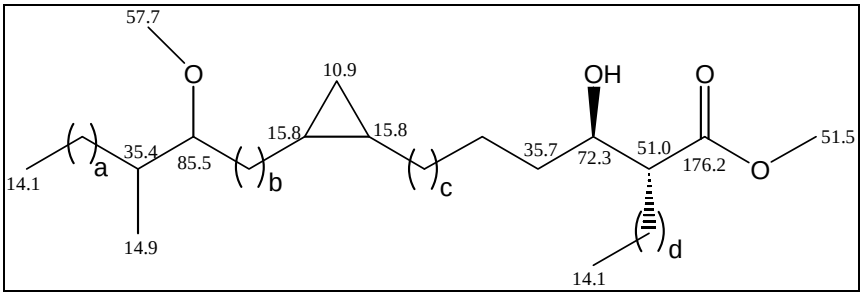


***Figure 2.13:*** *Methoxy mycolic acid methyl ester with $^{13}$C signals. Chemical shifts are quoted in δ relative to the trace resonance of $CDCl_3$ (δ 77.0 ppm).*

Figure 2.14 shows the ratios of one the *cis*-cyclopropane ring protons to the four ring protons of the *trans*-cyclopropane. The *trans*-cyclopropane was calculated to be less than 6%, Watanabe *et al*. the *cis*-cyclopropane to *trans*-cyclopropane ration to be 1:0.14 (150).

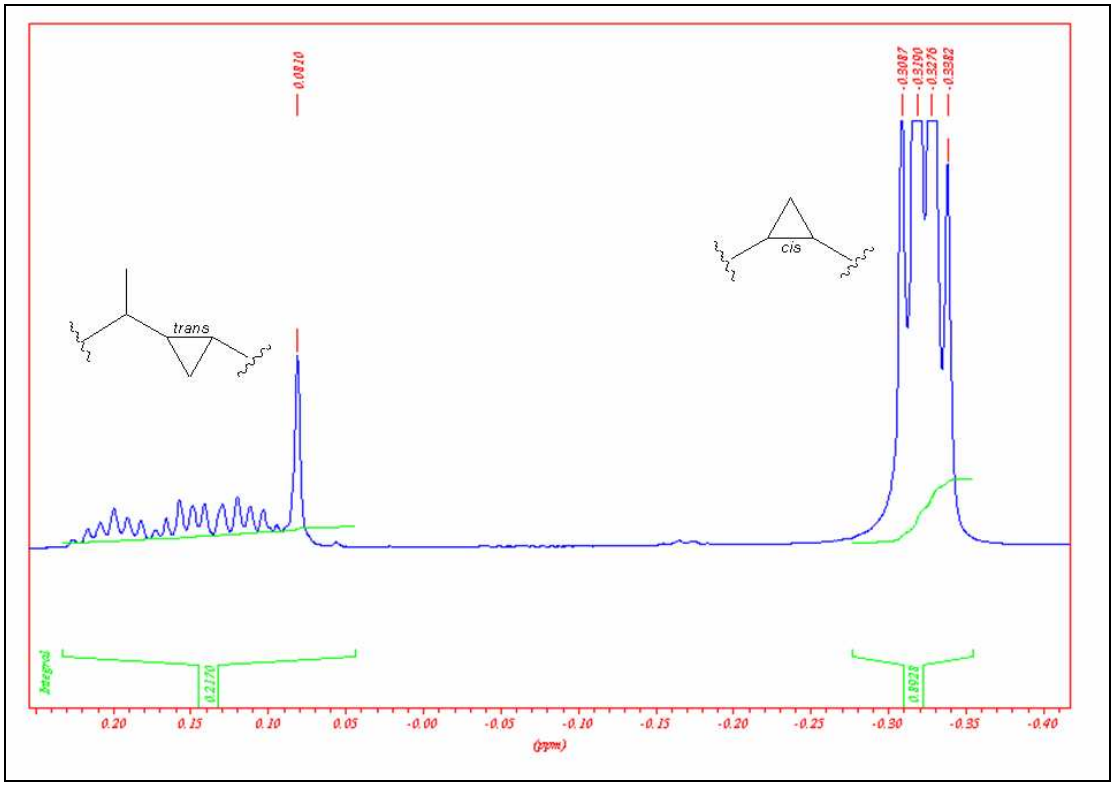


***Figure 2.14:*** *$^{1}$H NMR spectrum of methoxy mycolic acid methyl ester showing the trans-cyclopropane.*

The $^{1}$H NMR spectrum of the keto mycolic acid methyl ester showed a singlet at δ 3.72 for the methyl group in the mycolic acid motif. The β-proton appeared as a multiplet at δ 3.66 and the α-proton as a double of triplets at δ 2.44 (*J* 5.3, 9.2 Hz). The proton next to the keto-group appeared at δ 2.49. The *cis*-cyclopropane ring protons appeared as a multiplet at δ 0.65, a triplet of doublets at δ 0.57 (*J* 4.1, 8.2 Hz) and a double doublet at δ -0.33 (*J* 4.1, 5.3 Hz). The protons of the *trans*-cyclopropane ring appeared as multiplets at δ 0.45 and 0.02-0.0, the *trans*-cyclopropane was more than 10%. As shown in Table 2.4, a very small amount of the keto mycolic acid methyl ester was recovered; therefore the signals were not as strong as would have been ideal for interpretation (Figure 2.15). The $^{13}$C NMR spectrum included carbonyl signals at δ 215.3 and δ 176.20. The β-carbon appeared at δ 72.33, the α-carbon at δ 51.00 and the carbon of the methyl ester at δ 51.47. The spectrum showed signals for the *cis*-cyclopropane ring at δ 15.80 and 10.94 (Figure 2.16).

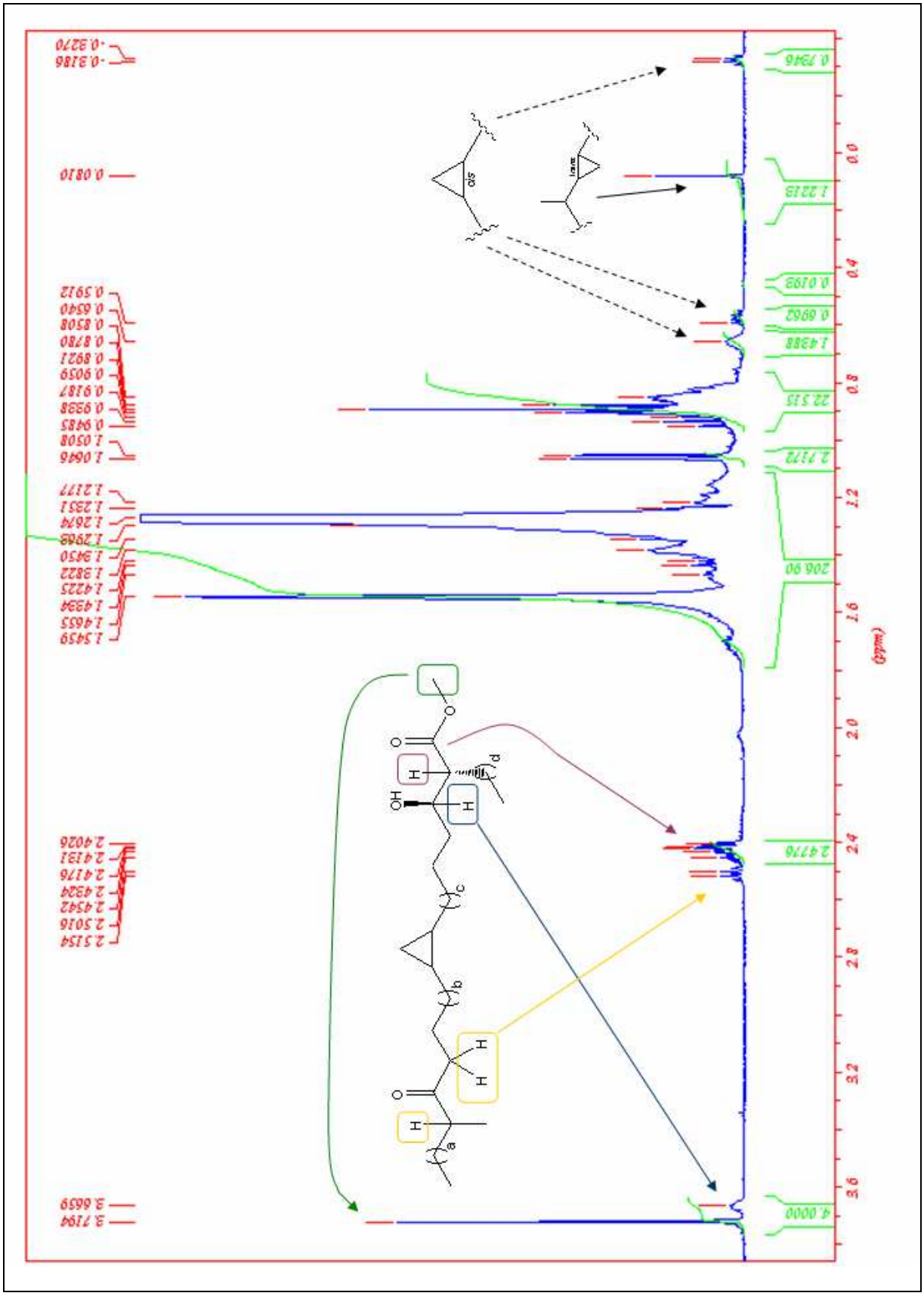

***Figure 2.15:*** *$^{1}$H NMR spectrum of keto mycolic acid methyl ester.*

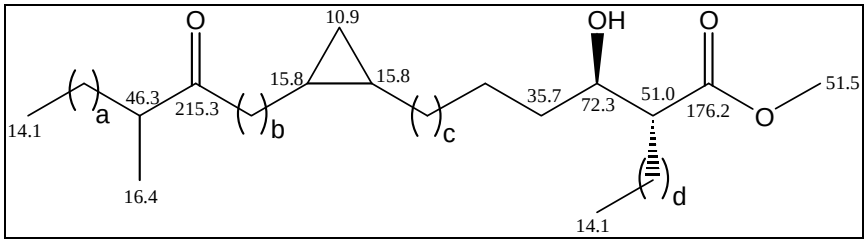


***Figure 2.16:*** *Keto mycolic acid methyl ester with $^{13}C$ signals. Chemical shifts are quoted in $\delta$ relative to the trace resonance of $CDCl_3$ ($\delta$ 77.0 ppm).*

Figure 2.17 shows the ratios of the four *trans*-cyclopropane ring protons to the four protons of the *cis*-cyclopropane ring in the keto mycolic acid methyl ester.

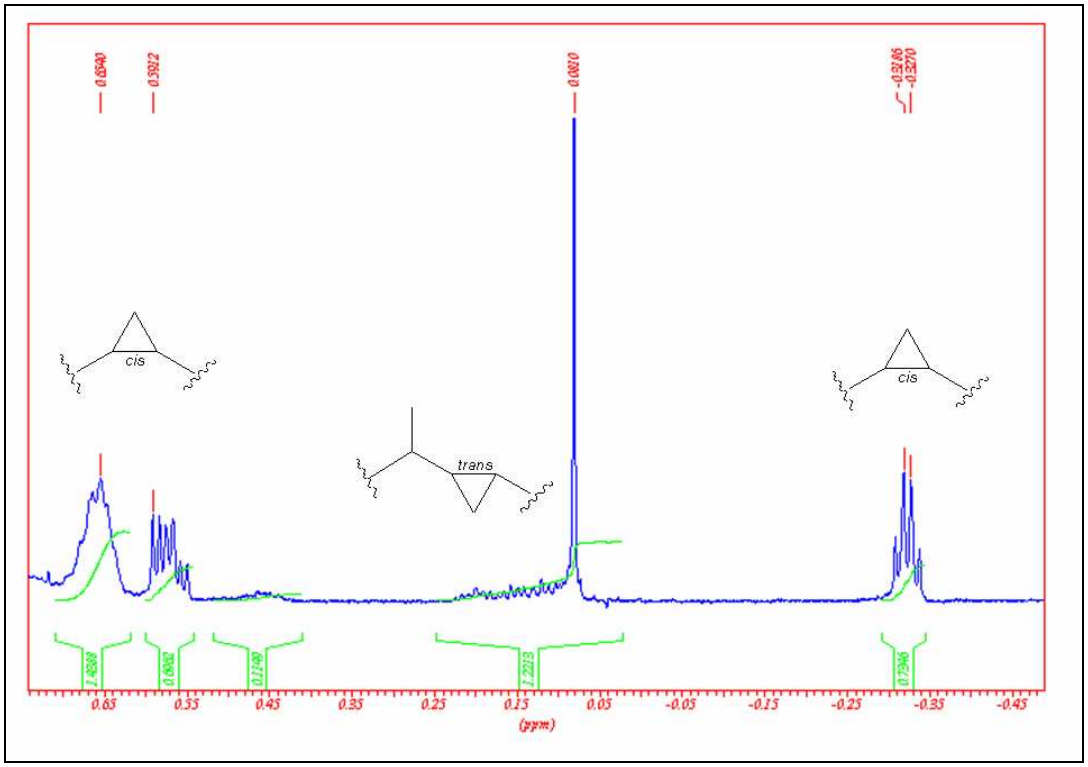


***Figure 2.17:*** *$^1H$ NMR spectrum of keto mycolic acid methyl ester showing trans-cyclopropane.*

Molecular weights of α-MA methyl esters, methoxy-MA methyl ester and keto-MA methyl esters were evaluated by MALDI-TOF/MS. The spectra obtained were in agreement with those reported in the literature (93). The pseudo-molecular mass of the major component of each subclass [M + $Na^+$] corresponded to 1174, 1290 and 1246 respectively, as shown in Figures 2.18, 2.19 and 2.20.

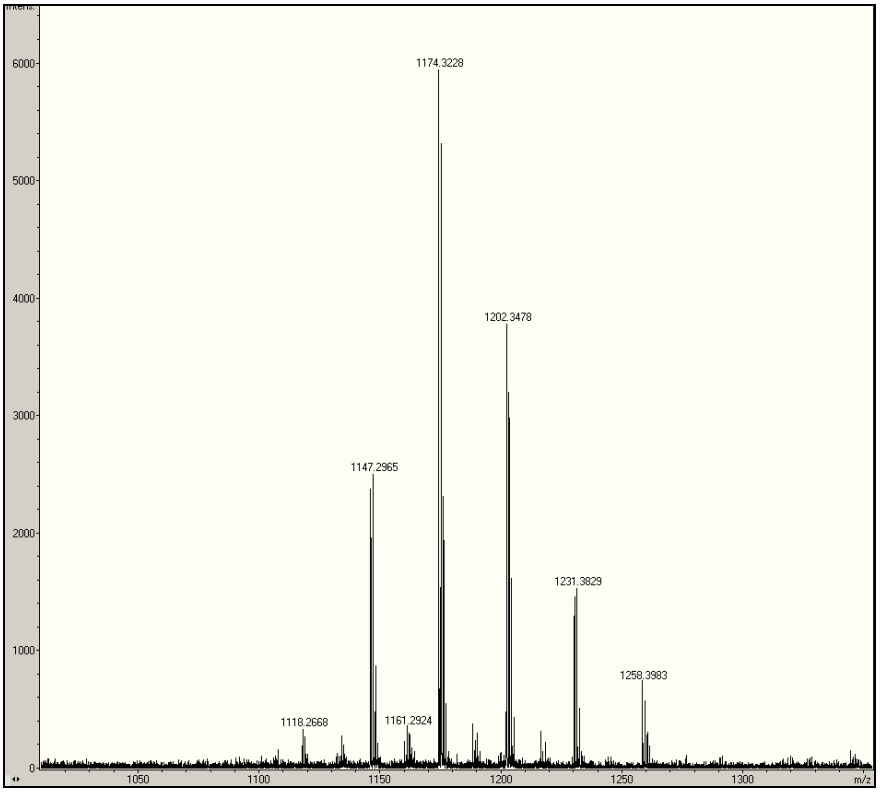


***Figure 2.18:*** *MALDI-TOF MS spectrum of α-MA methyl ester. The total carbon number of the free acid is 78.*

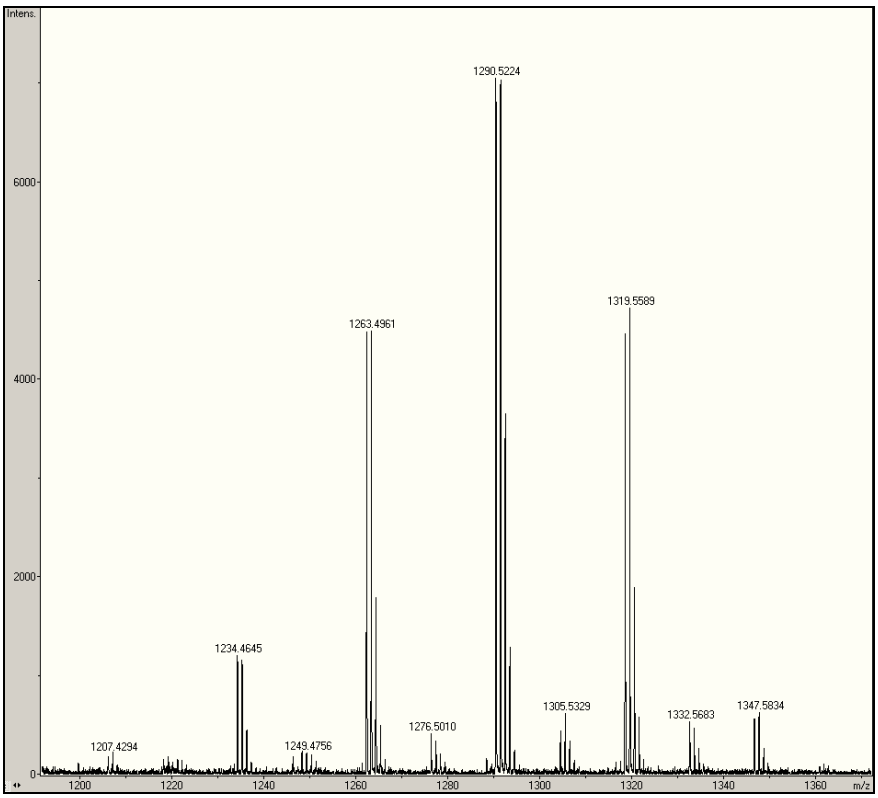


***Figure 2.19:*** *MALDI-TOF MS spectrum of methoxy-MA methyl ester. The total carbon number of the free acid is 85.*

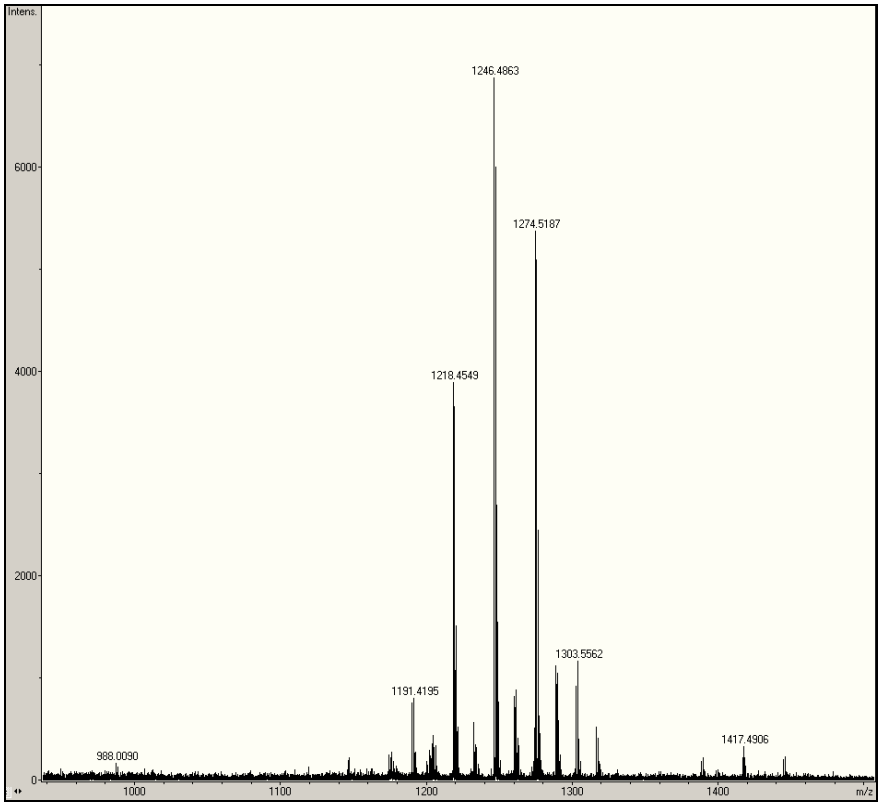


***Figure 2.20:*** *MALDI-TOF MS spectrum of keto-MA methyl ester. The total carbon number of the free acid is 82.*

## 2.3.2 Materials and methods

### *2.3.2.1 General considerations*

The MA sample was isolated from *M. tuberculosis* H37Rv and purified as described (67). HPLC was performed on a Phenomenex Luna 5 µ C18 column in a Merck Hitachi Chromatograph fitted with a Merck Hitachi L-4500 Diode Array Detector. NMR spectra were recorded either on a Bruker Advance 500 spectrometer with 5 mm BBO probe. Compounds analysed were solutions in deuterated chloroform ($CDCl_3$). All chemical shifts are quoted in δ relative to the trace resonance of protonated chloroform (δ 7.27 ppm) and $CDCl_3$ (δ 77.0 ppm). HPLC and NMR spectra were in agreement with the data reported in literature except that the sample contained some minor impurities (139, 150, 151).

### *2.3.2.2 Estimation of other components in natural mycolic acids*

A TLC was performed on Silica Gel 60 using petroleum ether/ethyl acetate (4/1, v/v); lipid spots were revealed by dipping the plates into a molybdophosphoric acid (10%) solution in ethanol, followed by heating. Quantification of individual spots was carried out on a Versadoc (Model 3000) imaging system. This confirmed that the sample contained less than 10% of impurities.

### *2.3.2.3 NMR analysis of the natural mycolic acids*

$\delta_H$: 3.34 (3H, s, CHOC<u>H</u>$_3$), 2.96 (1H, m, C<u>H</u>OCH$_3$), 2.44 (1H, dt, *J 5.4*, 8.9 Hz, C<u>H</u>(CH$_2$)$_{23}$CH$_3$), 1.8-0.7 (other H, multiplets including a d at δ 1.05, *J* 6.9 Hz, 3H, C<u>H</u>$_3$CHCO), 0.65 (2H, m, *cis*-cyclopropane), 0.57 (1H, ddd, *J* 4.1, 8.2 Hz, CH *cis*-cyclopropane), 0.4 (3H, m, *trans*-cyclopropane), 0.1 (1H, m, *trans*-cyclopropane), -0.33 (1H, broad dd, *J* 5.0, 8.9 Hz, *cis*-cyclopropane).

$\delta_C$: 176.21 (<u>C</u>O$_2$CH$_3$), 85.48 (<u>C</u>OCH$_3$), 72.33 (<u>C</u>HOH), 57.72 (CO<u>C</u>H$_3$), 51.48 (CO$_2$<u>C</u>H$_3$), 50.98 (<u>C</u>H(CH$_2$)$_{23}$CH$_3$), 35.59 (CH$_2$), 35.41 (<u>C</u>HCH$_3$), 32.43 (CH$_2$), 31.94 (CH$_2$), 31.59 (CH$_2$), 30.53 (CH$_2$), 30.22 (CH$_2$), 29.99 (CH$_2$), 29.94 (CH$_2$), 29.71 (CH$_2$), 29.58 (CH$_2$), 29.51 (CH$_2$), 29.43 (CH$_2$), 29.37 (CH$_2$), 28.74 (CH$_2$), 28.09 (CH$_2$), 27.57 (CH$_2$), 27.33 (CH$_2$), 26.17 (CH$_2$), 25.74 (CH$_2$), 22.69 (CH$_2$), 15.78 (CHcyclopropane), 14.88 (CH<u>C</u>H$_3$), 14.11 (CH$_3$), 10.91 (CH$_2$cyclopropane).

### *2.3.2.4 Esterification of mycolic acids*

To form the methyl esters, MAs (100 mg, ~ 0.1 mmol) were dissolved in a mixture of toluene:methanol (5:1, 18 ml). Thereafter trimethylsilyl diazomethane (TMDM, 2 M solution, Fluka, 0.2 ml, 0.4 mmol) was added, followed by further 4 additions of TMDM (0.1 ml, 0.2 mmol) every 45 minutes. The mixture was stirred for 72 hours, and then quenched by evaporation. The residue was dissolved in dichloromethane (15 ml) and water (10 ml) was added. The two layers were separated and the water layer extracted with dichloromethane (2 x 10 ml). The combined organic layers were dried and the solvent evaporated to give the desired compound (98 mg, ~ 97%). The NMR spectra of the compounds obtained, corresponded to those reported in the literature for methyl MAs (149, 150).

### *2.3.2.5 NMR analysis of the mycolic acids methyl esters*

$\delta_H$: 3.72 (3H, s, CO$_2$C<u>H</u>$_3$), 3.66 (1H, m, C<u>H</u>OH), 3.34 (3H, s, CHOC<u>H</u>$_3$), 2.95 (1H, m, C<u>H</u>OCH$_3$), 2.44 (1H, dt, J 5.4, 8.9 Hz, C<u>H</u>(CH$_2$)$_{23}$CH$_3$), 1.8-0.7 (other H, multiplets including a d at δ 1.05, *J* 6.9 Hz, 3H, C<u>H</u>$_3$CHCO), 0.65 (2H, m, *cis*-cyclopropane), 0.57 (2H, ddd, *J* 4.1, 8.2 Hz, CH *cis*-cyclopropane), 0.4 (m, *trans*-cyclopropane), 0.1 (m, *trans*-cyclopropane), -0.33 (1H, broad dd, *J* 5.0, 8.9 Hz, *cis*-cyclopropane).

$\delta_C$: 176.21 (<u>C</u>O$_2$CH$_3$), 85.48 (<u>C</u>OCH$_3$), 72.33 (<u>C</u>HOH), 57.72 (CO<u>C</u>H$_3$), 51.48 (CO$_2$<u>C</u>H$_3$), 50.98 (<u>C</u>H(CH$_2$)$_{23}$CH$_3$), 35.73 (CH$_2$), 35.40 (<u>C</u>HCH$_3$), 32.43 (CH$_2$), 31.93 (CH$_2$), 30.54 (CH$_2$), 30.22 (CH$_2$), 29.99 (CH$_2$), 29.95 (CH$_2$), 29.71 (CH$_2$), 29.51 (CH$_2$), 29.43 (CH$_2$), 29.37 (CH$_2$),

29.15 ($CH_2$), 28.74 ($CH_2$), 28.09 ($CH_2$), 27.58 ($CH_2$), 27.43 ($CH_2$), 26.18 ($CH_2$), 25.74 ($CH_2$), 22.69 ($CH_2$), 15.78 (CHcyclopropane), 14.88 ($CH\underline{C}H_3$), 14.11 ($CH_3$), 10.91 ($CH_2$cyclopropane).

### *2.3.2.6 Separation of the different subclasses of mycolic acids*

Separation of the different fractions of MAs was achieved by preparative TLC (Silica Gel 60, Merck) using the same procedures for elution and the revealing of the spots at the two extremities of the plates as described in section *2.3.2.2*. The mycolic acid methyl esters were eluted from the silica gel with dichloromethane. Then each fraction was purified by Flash column chromatography using Fluorosil (60-100 mesh, Aldrich) and eluting with a solution of petroleum ether:diethyl ether (9:1). This method proved efficient for the α-MA methyl ester and methoxy-MA methyl ester fractions, while the keto-MA methyl ester subclass was further purified by preparative TLC. The purity of the various types of mycolates was checked by analytical TLC, as described in section *2.3.2.2*.

### *2.3.2.7 Estimation of different subclasses of mycolic acids*

A TLC was performed on Silica Gel 60 developed in petroleum ether/ethyl acetate (4/1, v/v). Lipid spots were revealed by dipping the plates into a molybdophosphoric acid (10%) solution in ethanol, followed by heating. Quantification of individual spots was done on a Versadoc (Model 3000) imaging system.

### *2.3.2.8 NMR analysis of α-mycolic acid methyl esters*

$\delta_H$ (500 MHz): 3.72 (3H, s, $OC\underline{H}_3$), 3.66 (1H, m, $C\underline{H}OH$), 2.44 (1H, dt, *J* 5.3, 9.2 Hz, $C\underline{H}(CH_2)_{23}CH_3$), 1.8-1.0 (other H, m), 0.95-0.7 (other H, m), 0.65 (4H, m, $C\underline{H}$ *cis*-cyclopropane), 0.57 (2H, td, *J* 4, 8.2 Hz, CH *cis*-cyclopropane), -0.33 (2H, m, $C\underline{H}_2$ *cis*-cyclopropane).

$\delta_C$ (125.8 MHz): 176.20 ($\underline{C}O_2CH_3$), 72.32 ($\underline{C}HOH$), 51.47 ($CO_2\underline{C}H_3$), 51.00 ($\underline{C}H(CH_2)_{23}CH_3$), 35.73, 31.93, 29.71, 29.62, 29.59, 29.57, 29.51, 29.42, 29.36, 28.74, 27.43, 25.74, 22.69, 15.80 (CH *cis*-cyclopropane), 14.10 ($CH_3$), 10.94 ($CH_2$ *cis*-cyclopropane).

### *2.3.2.9 NMR analysis of methoxy mycolic acid methyl esters*

$\delta_H$ (500 MHz): 3.72 (3H, s, $OC\underline{H}_3$), 3.66 (1H, m, $C\underline{H}OH$), 3.32 (3H, s, $CHOC\underline{H}_3$), 2.96 (1H, m, $C\underline{H}OCH_3$), 2.44 (1H, dt, *J* 5.3, 9.2 Hz, $C\underline{H}(CH_2)_{23}CH_3$), 3.72 (3H, s, $OC\underline{H}_3$), 3.66 (1H, m,

CHOH), 2.44 (1H, dt, *J* 5.3, 9.2 Hz, CH$(CH_2)_{23}CH_3$), 1.8-1.0 (other H, m), 0.95-0.7 (other H, m), 0.65 (2H, m, CH *cis*-cyclopropane), 0.57 (1H, td, *J* 4, 8.2 Hz, CH *cis*-cyclopropane), 0.45 (1H, m, CH-*trans*-cyclopropane, less than 6%), 0.2-0.0 (3H, m, *trans*-cyclopropane), -0.33 (1H, m, $CH_2$ *cis*-cyclopropane).

$\delta_C$ (125.8 MHz): 176.20 ($CO_2CH_3$), 85.47 ($COCH_3$), 72.32 (CHOH), 57.71 ($COCH_3$), 51.47 ($CO_2CH_3$), 51.00 (CH$(CH_2)_{23}CH_3$), 38.2 ($CHCH_3$ *trans*-cyclopropane) 35.73, 35.41, 32.43, 31.93, 30.54, 29.92, 29.71, 29.61, 29.57, 29.50, 29.43, 29.36, 28.73, 27.59, 27.44, 26.16 (CH *trans*-cyclopropane), 22.69 ($CH_2$), 2.16, 19.72 ($CH_3CH$), 18.62 (CH *trans*-cyclopropane), 15.80 (CH *cis*-cyclopropane), 14.88 ($CHCH_3$ *trans*-cyclopropane), 14.10 ($CH_3$), 10.94 ($CH_2$ *cis*-cyclopropane), 10.54 ($CH_2$ *trans*-cyclopropane).

### *2.3.2.10 NMR analysis of keto mycolic acid methyl ester*

$\delta_H$ (500 MHz): 3.72 (3H, s, $OCH_3$), 3.66 (1H, m, CHOH), 2.49 (1H, q, *J* 6.9 Hz, $COCHCH_3$), 2.44 (1H, dt, *J* 5.3, 9.2 Hz, CH$(CH_2)_{23}CH_3$), 2.41 (2H, td, *J* 1.8, 7.0 Hz, $CH_2CO$), 1.8-1.0 (other H, multiplet including a d at δ 1.05, *J* 6.9 Hz, 3H, $CH_3CH$), 0.65 (2H, m, CH *cis*-cyclopropane), 0.57 (1H, ddd, *J* 4.1, 8.2 Hz, CH *cis*-cyclopropane), 0.45 (1H, m, CH *trans*-cyclopropane, more than 10%), 0.2-0.0 (3H, m, *trans*-cyclopropane), -0.33 (1H, dd, *J* 4.1, 5.3 Hz, $CH_2$ *cis*-cyclopropane).

$\delta_C$ (125.8 MHz): 215.3 (C=O), 176.20 ($CO_2CH_3$), 72.33 (CHOH), 51.47 ($CO_2CH_3$), 51.00 (CH$(CH_2)_{23}CH_3$), 46.35, 41.14, 35.73, 31.93, 30.23, 29.70, 29.50, 29.43, 29.36, 28.73, 27.44, 27.34, 23.75, 22.69, 16.36 ($CHCH_3$ keto-group), 15.80 (CH *cis*-cyclopropane), 14.10 ($CH_3$), 10.94 ($CH_2$ *cis*-cyclopropane).

### *2.3.2.11 MALDI-TOF Mass Spectrometry*

Dried samples (5 mg) were redissolved in 1.0 ml of chloroform. An aliquot was mixed with an equal volume of 2,5 dihydroxybenzoic acid (2,5-DHB) matrix solution [10 mg/ml 2,5-DHB in chloroform : methanol (1:1)] and 0.7 µl spotted onto a MALDI target that had been seeded with a layer of 2,5-DHB (in ethanol). Mass spectra were acquired in reflectron mode with delayed ion extraction using 40 laser shots per acquisition. Between 120 and 160 laser shots were accumulated into the final summed spectrum. Spectra were externally calibrated using a peptide mixture in CHCA matrix (93).

## 2.4 Biological activity/antigenicity of subclasses of mycolic acids

### 2.4.1 Results and discussion

After a few attempts, the natural MA was successfully separated into the different subclasses and purified. The next step was to determine the biological activity/antigenicity of these different subtypes by using ELISA. Pan *et al.* (112) showed that by using ELISA, the methoxy-MA was recognised better than the α- and keto-MA by sera from TB positive patients. They applied the MAs as methyl esters in *n*-hexane solution to the ELISA plate wells.

With ELISA being the easiest and quickest way to obtain results for antibody recognition against certain antigens, ELISA plate wells were coated with MAs as methyl esters and as free acids in chloroform, as shown in Figure 2.21. MA had to be esterified in order to be separated into the different subclasses. However, the methyl esters were not recognised by antibodies in $TB^+$ patient serum, therefore the hydrolysis (de-esterification) of the different subclasses was required. Pan *et al.* (112) and Fujita *et al.* (64) showed that cord factor was recognised by antibodies in $TB^+$ patient serum. Cord factor was therefore included as control.

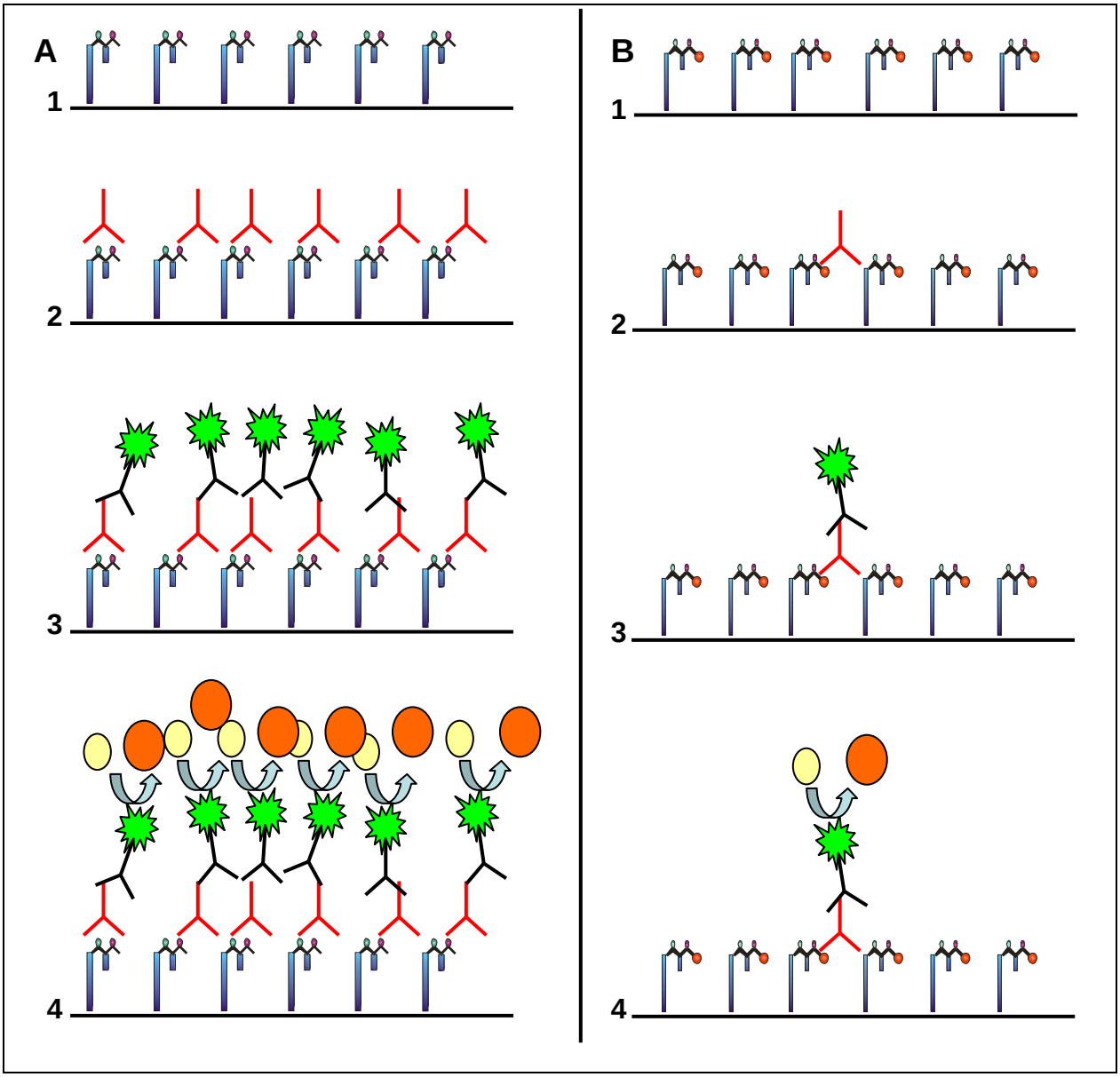


***Figure 2.21:*** *Schematic presentation of ELISA.* ***A*** *shows results of antibody binding to the antigen (in this case natural MA).* ***B*** *shows the results of no antibody binding to the antigen (in this case MA methyl ester). 1. Coating with antigen. 2. Incubation with serum. 3. Addition of conjugate and 4. Addition of substrate and monitoring of colour change.*

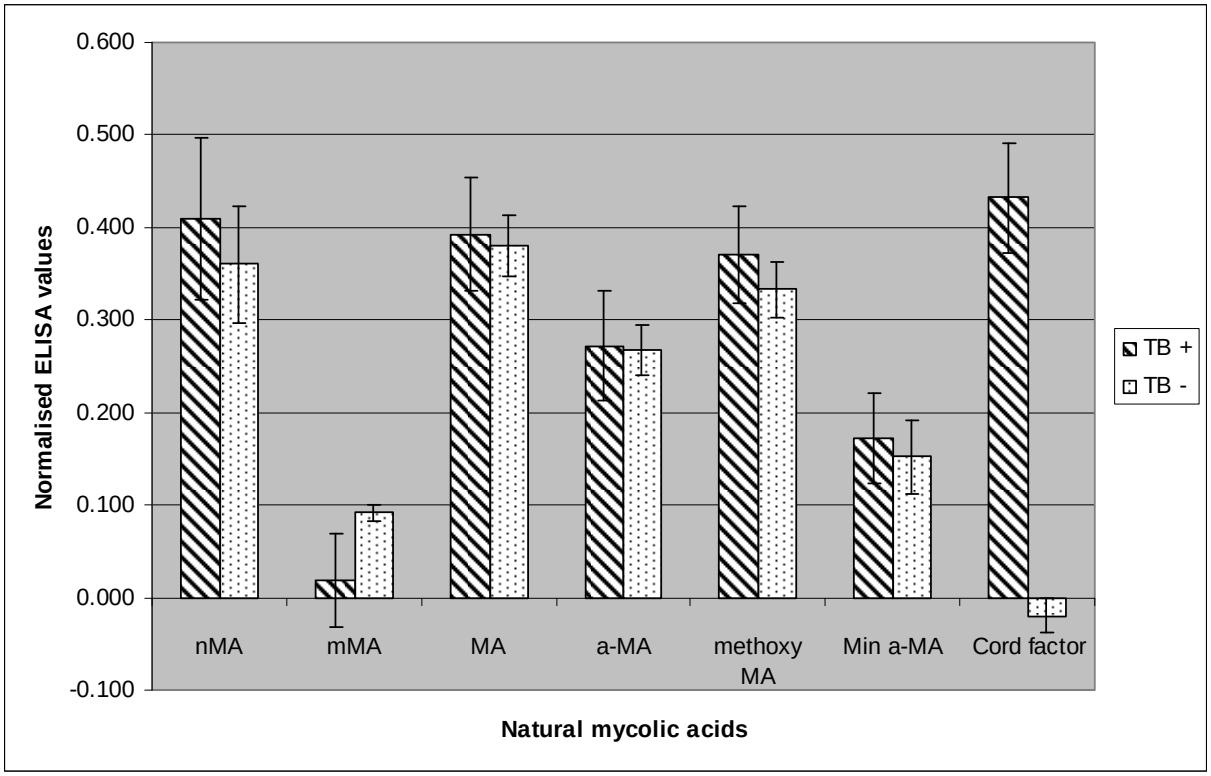


***Figure 2.22:*** *ELISA results of antibody binding to natural MA (nMA, n=92), natural mycolic aicd methyl esters (mMA, n=20), MA (MA, n=18), alpha-MA (α-MA, n=20), methoxy-MA (methoxy-MA, n=20), α-MA (Min α-MA, n=20) and cord factor (n=20). The source of the antibodies was sera collected from either TB positive, kindly provided by Dr AC Stoltz from the Pretoria Academic Hospital, or TB negative South African hospitalised patients of various adult age groups* (127). *(Values are given as a mean ± standard deviation).*

Figure 2.22 summarises the results obtained with ELISA. $TB^+$ patient serum gave a relatively strong signal against natural MA (nMA) and cord factor, as well as against the MA (MA) and methoxy-MA (methoxy-MA), but weaker signals against the α-MA (α-MA) and the α-MA (Min α-MA). $TB^+$ patient serum did not recognise the methylated MA (mMA).

$TB^-$ patient serum, just like $TB^+$ sera, also recognised MA (nMA), MA, alpha-MA, methoxy-MA and the alpha-MA (Min α-MA), and it also did not give a signal against the esterified MA (mMA). Interestingly, however, $TB^-$ patient serum did not recognise cord factor, which gave among the strongest of signals with $TB^+$ sera.

Statistically (Student's t test), compared to MA, there was no significant difference in the binding of $TB^+$ patient serum antibodies to MA, methoxy-MA or to cord factor. Antibody binding to the methylated MA was very low compared to natural MA. The ELISA signal against the alpha-MA was much higher compared to the esterified MA, but significantly lower

compared to natural MA ($P < 0.0001$). Antibodies recognised the natural MA (Min α-MA) a little less than the MA, but significantly less than methoxy-MA ($P < 0.0001$).

Closer analyses of $^{1}H$ NMR spectra of both separated natural alpha-MA (Figure 2.11) and natural alpha-MA from Prof D.E. Minnikin (University of Birmingham, UK) showed a small amount of methoxy-MA present. This might explain the signals obtained against these antigens, as the more hydrophilic oxygenated MA may preferentially orientate itself in the antigen coat to be more accessible for antibody binding than the majority of α-MA.

The results found contradicted that reported by Pan and his co-workers (112). We found that the methyl esters of the MAs were not recognised by TB positive patient serum in the ELISA assay. Pan *et al.* (112) showed recognition of the methoxy-MA methyl esters. This might be due to small differences in the method followed by Pan *et al.*, and the method used for this study. Pan *et al.* coated the ELISA plate wells with MA methyl esters in *n*-hexane and used 0.05% Tween-20 in PBS as blocking solution, whereas in this study the MA methyl esters and free MA were coated from hot PBS solutions, while 0.5% casein in PBS was used as blocking solution. Deposition of MA from an aqueous, rather than a hydrophobic environment, may influence the conformation assumed by the immobilised MA.

Esterified MA was used as negative control in order to prove that a specific conformation, which can be destroyed by the elimination of the hydrogen bonding capacity of the carboxylic acid in the α- and the hydroxyl group in β-position, is important for defining the "cholesteroid" nature of MAs. The formation of a hydrogen bond between the α-carboxylic and the β-hydroxyl of MA is particularly stable for the natural *erythro* configuration of *2R,3R* 2-alkyl,3-hydroxy acids and has been shown to have a stabilising effect on the alignment of the alkyl chains affecting the physical properties of these acids (52, 53). Sugar esters, such as trehalose mono- or dimycolates, may also suffice to stabilise the folding of the mero chain by hydrogen bonding, as it retains hydroxyl groups in the vicinity of the α-carboxylic group of MA, but the methyl ester of MA substitutes the hydrogen atom on the carboxylic acid with a hydrophobic moiety that has no possibility for hydrogen bonding with the oxygenated group of the mero chain. This may explain why the recognition of cord factor by $TB^{+}$ patient serum was still allowed, despite the esterification of the mycolates. In corroboration of the results obtained here, Grant *et al.* (70) reported that the ability of the T-cell antigen receptor to recognise MA

presented to the T-cell on the CD1b protein of an antigen presenting cell was abolished when the methyl ester of MA was presented instead.

The loss of antigenicity of the mycolic acid methyl ester indicated that the mycolic motif plays an important role in recognition by antibodies. The importance of the mero chain was shown by the difference in antibody recognition of the alpha-MA and the methoxy-MA.

From these results it is clear that both the mycolic motif and the mero chain play and important role in antigenicity of MAs.

Much can be learned from the different results obtained with $TB^+$ and $TB^-$ patient sera against cord factor, as opposed to the similar signals that were obtained with $TB^+$ and $TB^-$ patient sera against all the free hydroxy acid MAs. With cord factor, only $TB^+$ patient sera showed recognition, whereas $TB^-$ patient serum did not recognise cord factor at all. The results can be interpreted in a way similar to that applied to the antigenicity of virus particles of the development of subcomponent vaccines for viral diseases in humans and animals (144).

In the case of viruses, different types of virus particles are secreted from infected cells that will be recognised by antibodies of the host. Virus particles also self-assemble with different virus particles into whole or partial virus coats and these may also be brought into contact with the immune system during the course of infection. In this way, three categories of antigenic epitopes may be recognised per virus particle that are necessary to explain the immune phenomena that are observed. These categories are metatopes, cryptotopes and neotopes. Metatopes are antigenic epitopes that are recognised on both individual virus particles and on the same particle that has been wholly or partially self-assembled into virus coats. Cryptotopes are types of epitopes occurring on the facet of the virus particle that is obscured by self-assembly with other virus particles. These epitopes are therefore hidden from interaction with antibodies, hence the name *crypto*-tope. When two viral particles combine, they may create a single epitope that spans over both particles, thereby creating a new epitope (neotope) that cannot be recognised on either of the two particles alone before their assembly into a single antigenic entity. This concept is illustrated in Figure 2.23.

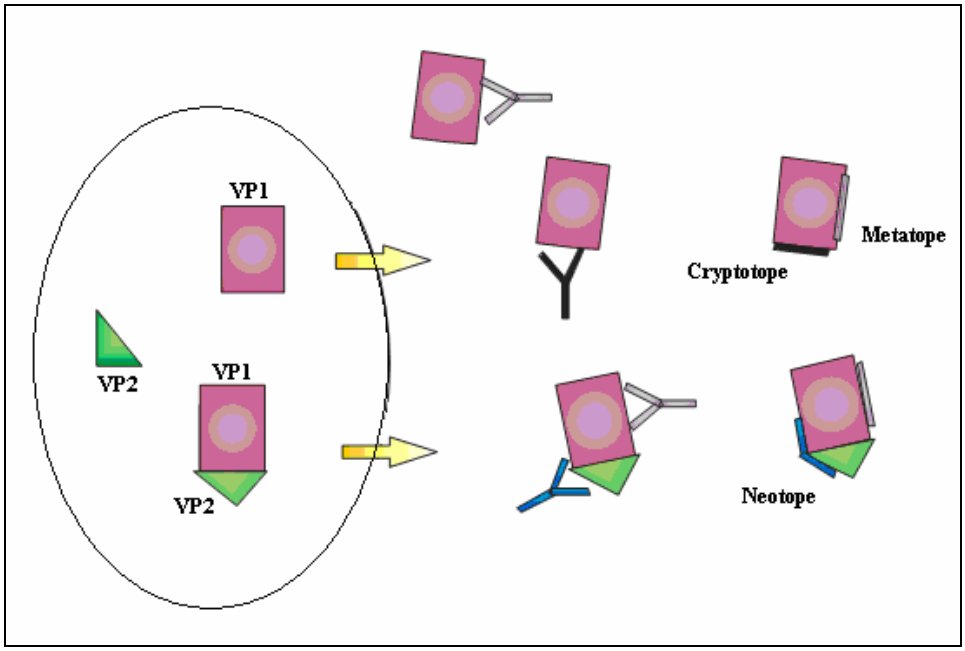


***Figure 2.23:*** *Cartoon drawing of the different viral epitopes that are formed in the host cell and are recognised by different antibodies when secreted from the infected cell: cryptotope in black, metatope in lilac and neotope in blue.*

By analogy to the above figure, insight can be gained in the antibodies from $TB^+$ and $TB^-$ patients recognising MAs and cord factor. The MA might have a cryptotope that can be recognised by anti-MA antibodies, as well as by anti-cholesterol antibodies that occur in all humans at different levels of expression and affinity. When MAs are linked to trehalose to form cord factor, this epitope might be hidden (cryptotope) and a new epitope (neotope) might form, one that can then only be recognised by anti-cord factor antibodies that occur in $TB^+$, but not in $TB^-$ patient sera (Figure 2.24). The results imply that free MA may not be very useful in the serodiagnosis of TB, at least not when ELISA is used as the immunoassay. In contrast, cord factor appears as a very strong candidate to base TB serodiagnosis on. This finding corroborates the results reported by Fujita *et al.* in 2005 (64).

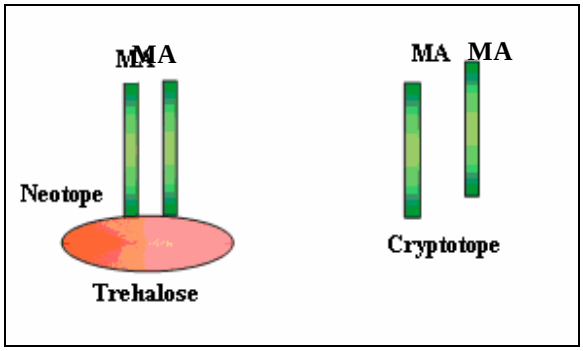


***Figure 2.24:*** *Possible epitopes in MAs and cord factor that are recognised by different antibodies.*

## 2.4.2 Materials and methods

### *2.4.2.1 Mycolic acids used as antigens*

#### *2.4.2.1.1 Natural MA (nMA)*

Natural MA was isolated from *M. tuberculosis* H37Rv, as described by Goodrum *et al.* (67), as a mixture of α-, keto- and methoxy-MAs as shown in Figure 1.7.

#### *2.4.2.1.2 Natural mycolic aicd methyl esters (mMA)*

Natural MA had to be esterified in order to be separated into the different subclasses. The COOH was methylated (67) to give COOMe as shown in Figure 2.25.

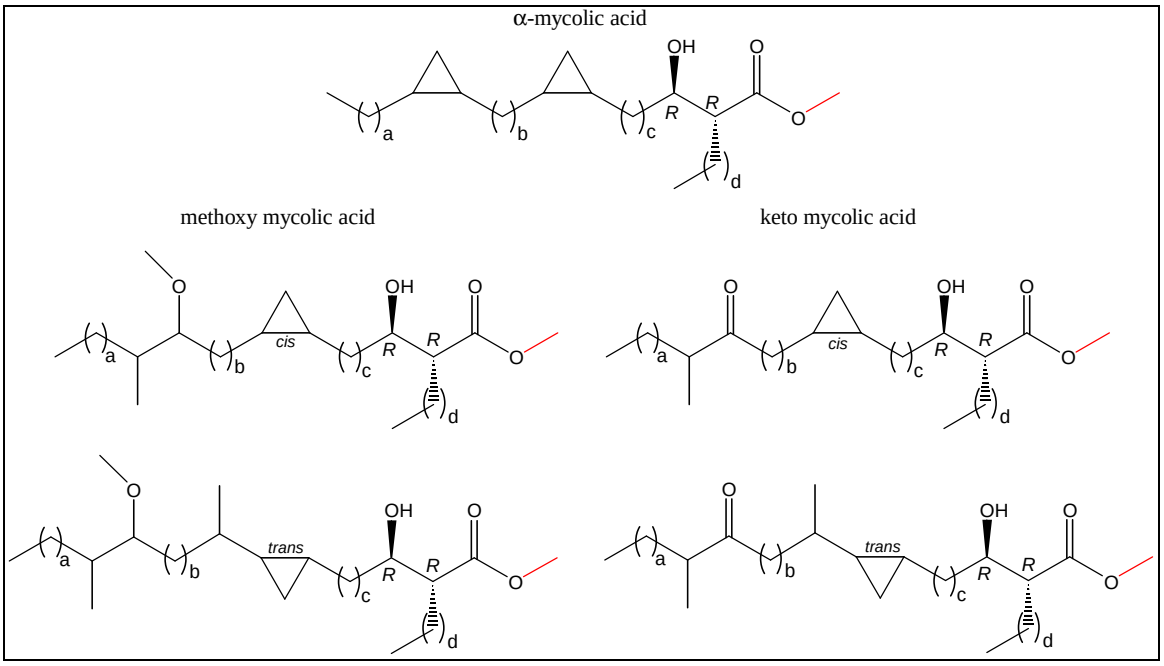


***Figure 2.25:*** *Natural mycolic acid methyl esters.*

#### *2.4.2.1.3 Mycolic acids (MA)*

The methyl group from the natural mycolic acid methyl ester was removed by dissolving MA (10 mg) in a solution of potassium hydroxide and propan-2-ol (100 mg/ml, 1 ml). The mixture was stirred at 85 ºC for 3½ hours. The reaction was quenched by adding water (1 ml) and the MA was extracted 15 times with hexane. The organic layers were collected and dried over anhydrous calcium chloride, filtered and the hexane evaporated.

*2.4.2.1.4 Alpha-MA (α-MA) and methoxy-MA (methoxy-MA)*

The methylated natural MA was separated into the different subclasses and each subclass was demethylated as described in section *2.4.2.1.3*.

*2.4.2.1.5 Natural alpha-MA from Prof Minnikin (Min α-MA)*

Natural deprotected α-MA, from *M. tuberculosis*, was kindly provided by Prof D.E. Minnikin (University of Birmingham, UK). $^{1}$H NMR showed minute amounts (about 1%) of methoxy-MA.

*2.4.2.1.6 Cord factor (Trehalose-6,6'-dimycolate)*

Commercial cord factor (Fig 2.26) was bought from Sigma, (Steinheim, Germany).

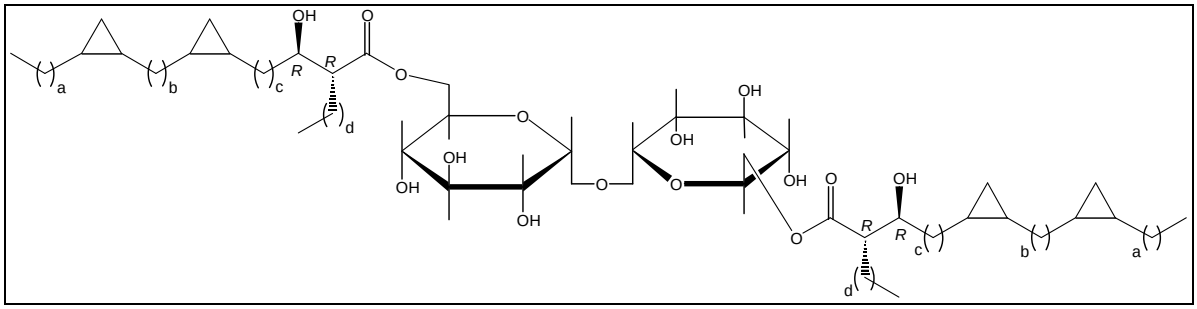


***Figure 2.26:*** *Cord factor.*

***2.4.2.2 Reagents and apparatus used in ELISA***

ELISA plates: flat bottom, 96 wells (Bibby Sterilin Ltd., Sterilab, UK).

Phosphate buffered saline (PBS): 20 x PBS stock was prepared by dissolving sodium chloride (160 g; 99%, Merck, SA), potassium chloride (4 g; 99%, Merck, SA), di-hydrogen potassium phosphate (4 g, 99%, Merck, SA) and di-sodium hydrogen phosphate (23 g; 99%, Merck, SA) in double distilled de-ionized water to a final volume of 1000 ml.

PBS (1 x): 50 ml of the 20 x PBS solution was diluted in 950 ml ddd$H_2O$. The pH of the solution was adjusted to 7.4 with 1 M NaOH.

Casein-PBS (0.5%): 5 g of casein (0.1% fat, 0.1% fatty acids; Merck, SA) were dissolved in a final volume of 1000 ml PBS by stirring at 37 °C for 2 hours. The pH was adjusted to 7.4 with 1 M sodium hydroxide and then stored at 4 °C overnight for use within the next day.

Goat anti-human IgG peroxidase conjugate: A 1/1000 dilution of the conjugate was prepared by adding peroxidase conjugate (10 µl; whole molecule, Sigma, Steinheim, Germany) to 0.5% casein PBS (10 ml) five minutes prior to use.

*O-Phenylenediamine* (OPD): (Sigma, St. Louis, MD, USA).
Hydrogen peroxide ($H_2O_2$): Tablets of urea, 33-35% per gram (Sigma, St. Louis, MD, USA).

0.1 M Citrate buffer: citric acid (0.1 M, 450 ml; Sigma, USA) was added to citrate tri-sodium (0.1 M, 450 ml; Sigma USA) until a pH of 4.5. The solution was brought to a final volume of 1000 ml with double distilled de-ionized water.

#### *2.4.2.3 Human sera*

TB positive, HIV positive, patient serum was kindly provided by Dr. A.C. Stoltz, Pretoria Academic Hospital, Pretoria, South Africa. TB negative, HIV negative, hospitalized patient serum were kindly provided by Dr. G. Schleicher, Helen Joseph Hospital, Auckland Park, Johannesburg, South Africa (127).

#### *2.4.2.4 Preparation of coating solutions*

The antigens were heated in PBS buffer (4 ml) for 20 minutes at 85 ºC on a heatblock. The hot solutions were vortexed for 10 seconds and sonified (Virsonic 600 – Ultrasonic cell disrupter, United Scientific, New York, USA), output level 2, 1 minute, 30 sec on and 30 sec off). The plates were coated by adding the hot solutions at 50 µl per well and storing at 4 ºC overnight. The final antigen load was approximately 3 µg/well for MAs. PBS was included as control. Coating of the wells was confirmed under the microscope as visible fatty deposits adsorbed on the polystyrene.

#### *2.4.2.5 Blocking step*

After 16 hours of incubation with antigen solution, the plates were aspirated and blocked with casein-PBS (400 µl per well) for 2 hours at room temperature.

#### *2.4.2.6 Antibody binding*

The blocking solution was aspirated before the serum was added (TB positive and TB negative, 1:20 dilution in casein-PBS, 50 µl per well). The plates were incubated for 1 hour at

room temperature, then washed with casein-PBS (3 times) using the ELISA plate washer (Anthos Autowash automatic ELISA plate washer, Labsystems) and aspirated.

#### *2.4.2.7 Addition of conjugate and substrate*

The goat anti-human IgG peroxidase conjugate (50 µl per well) was added and incubated for 30 minutes at room temperature. The plates were then washed with casein-PBS (3 times) and aspirated. The substrate solution (10 mg OPD, 8 mg $H_2O_2$ in 10 ml citrate buffer) was prepared immediately before use and added to the plates (50 µl per well). The plates were incubated at room temperature and the colour development was monitored at 10, 30, 40 and 50 minutes after addition of the substrate using a photometer (SLT 340 ATC photometer, Thermo-Labsystems, Finland) at wavelength of 450 nm.